Springer
the language of science

Dear Author/Editor,

Here are the proofs of your chapter as well as the metadata sheets.

Metadata

- Please carefully proof read the metadata, above all the names and address.
- In case there were no abstracts for this book submitted with the manuscript, the first 10-15 lines of the first paragraph were taken. In case you want to replace these default abstracts, please submit new abstracts with your proof corrections.

Page proofs

- Please check the proofs and mark your corrections either by
  - entering your corrections online
    or
  - opening the PDF file in Adobe Acrobat and inserting your corrections using the tool "Comment and Markup"
    or
  - printing the file and marking corrections on hardcopy. Please mark all corrections in dark pen in the text and in the margin at least ¼" (6 mm) from the edge.
- You can upload your annotated PDF file or your corrected printout on our Proofing Website. In case you are not able to scan the printout , send us the corrected pages via fax.
- Please note that any changes at this stage are limited to typographical errors and serious errors of fact.
- If the figures were converted to black and white, please check that the quality of such figures is sufficient and that all references to color in any text discussing the figures is changed accordingly. If the quality of some figures is judged to be insufficient, please send an improved grayscale figure.

Metadata of the chapter that will be visualized online

Book Title		Developments in Medical Image Processing and Computational Vision
Chapter Title		Visual Pattern Recognition Framework Based on the Best Rank Tensor Decomposition
Copyright		Springer International Publishing Switzerland 2014
Corresponding Author	Family name	**Cyganek**
	Particle	
	Given name	**B.**
	Suffix	
	Division	
	Organization	AGH University of Science and Technology
	Address	Al. Mickiewicza 30, 30-059 Krakow, Poland
	email	cyganek@agh.edu.pl
Abstract		In this paper a framework for visual patterns recognition of higher dimensionality is discussed. In the training stage, the input prototype patterns are used to construct a multidimensional array—a tensor—whose each dimension corresponds to a different dimension of the input data. This tensor is then decomposed into a lower-dimensional subspace based on the best rank tensor decomposition. Such decomposition allows extraction of the lower-dimensional features which well represent a given training class and exhibit high discriminative properties among different pattern classes. In the testing stage, a pattern is projected onto the computed tensor subspaces and a best fitted class is provided. The method presented in this paper, as well as the software platform, is an extension of our previous work. The conducted experiments on groups of visual patterns show high accuracy and fast response time.

Visual Pattern Recognition Framework Based on the Best Rank Tensor Decomposition

B. Cyganek

Abstract In this paper a framework for visual patterns recognition of higher dimensionality is discussed. In the training stage, the input prototype patterns are used to construct a multidimensional array—a tensor—whose each dimension corresponds to a different dimension of the input data. This tensor is then decomposed into a lower-dimensional subspace based on the best rank tensor decomposition. Such decomposition allows extraction of the lower-dimensional features which well represent a given training class and exhibit high discriminative properties among different pattern classes. In the testing stage, a pattern is projected onto the computed tensor subspaces and a best fitted class is provided. The method presented in this paper, as well as the software platform, is an extension of our previous work. The conducted experiments on groups of visual patterns show high accuracy and fast response time.

1 Introduction

Recognition of patterns in different types of visual signals belongs to difficult computer tasks. Most problematic is high dimensionality of input data, as well as development of the methods of extraction of the features (a model) which well represent a given class of patterns and are sufficiently discriminative among the other. There are also some additional constraints superimposed on patter recognition methods, such as real-time operation or special platforms or conditions of operation. When analyzing different types of visual signals it becomes evident that a difficulty also comes from specific properties of different groups of images. For instance, the surveillance video may not be of well quality and the objects might be only partially seen and with high noise. On the other hand, medical images, such as radiograph images, may be of low contrast. All these scenarios cause research and engineering problems when designing pattern recognition systems. Frequently, additional expert knowledge is included into a design which results in highly specialized visual pattern recognition systems which are specialized in recognizing only specific types of objects. In this respect achievements in other disciplines frequently are of help.

B. Cyganek (✉)
AGH University of Science and Technology, Al. Mickiewicza 30, 30-059 Krakow, Poland
e-mail: cyganek@agh.edu.pl

J. M. R. S. Tavares, R. Natal Jorge (eds.), *Developments in Medical Image Processing and Computational Vision,* Lecture Notes in Computational Vision and Biomechanics 19,
DOI 10.1007/978-3-319-13407-9_6

Book ID: 329170_1_En ChapterID: 6 Dispatch Date: 12-01-2015 Proof No: 1

In this paper a method of pattern recognition in visual data is discussed with special stress on medical and biometric images and videos. The presented method is based on the best rank tensor decomposition and extends its version presented in our previous publication [4]. In this group of method, object recognition is accomplished by comparing distances of the lower-dimensional features obtained by projecting a test pattern into the best rank tensor subspaces of different pattern classes. The method was tested on the maxillary radiograph images and showed high accuracy and fast computation time. In this paper we follow this presentation and show additional aspects of the method. Specifically, the new pattern recognition framework was modified as compared to the method presented in [4]. In [4] it was proposed to select one of the best fitted prototypes for comparison. On the other hand, in this paper a modified version is proposed which account for impact of all prototype patterns which influence is averaged, as will be discussed. Also, the experimental results were extended onto the face recognition problem which builds into the biometric recognition framework.

The rest of this paper is organized as follows. In Sect. 2 the problem of pattern recognition with decompositions of pattern tensors is presented. Specifically, Sect. 2.1 presents an overview of pattern representation in the framework of best-rank prototype pattern decomposition, whereas in Sect. 2.2 pattern classification with the best rank tensor decomposition is discussed. Section 3 presents implementation details of the best rank tensor decomposition. In Sect. 4, the experimental results are presented and discussed. Finally, the paper ends with conclusions, presented in Sect. 5, as well as bibliography.

2 Pattern Recognition with the Pattern Tensor Decompositions

Recently, multidimensional arrays of data, called tensors, were proposed for pattern recognition. These, especially well fit into the problem of pattern recognition in visual signals due to a direct representation of each of the dimensions of the input signal.

Even more important are the methods of analyzing tensor content. In this respect a number of tensor decomposition methods were proposed [5, 10–12, 16]. In this respect the three decomposition methods are as follows.

1. The Higher-Order Singular Value Decomposition (HOSVD) [11].
2. The best rank-1 [12].
3. The best rank-(R_1, R_2, . . ., R_K) approximations [12, 16].

First of the above, the HOSVD can be used to build the orthogonal space for pattern recognition [14]. Its variant operating on tensors obtained from the geometrically deformed prototype patterns is discussed in [5]. However, HOSVD is not well suitable for data reduction. Although there is a truncated version HOSVD, its results lead to excessive errors. Thus, usually a truncated HOSVD is treated only as a coarse approximation or it can serve as an initialization method for other decompositions.

In terms of dimensionality reduction, better results can be obtained with the best rank-1 decomposition [12]. However, the best rank-(R_1, R_2, . . ., R_K) approximation offers much better behavior in terms of pattern representation in lower-dimensional subspaces, as shown by de Lathauwer [12], as well as other researchers, such as Wang and Ahuja [16]. In this paper we follow this approach, discussing its properties and a method of pattern recognition, as well as providing an experimental and software framework for pattern recognition with the best rank tensor decomposition.

2.1 *Pattern Representation in the Framework of Best-Rank Prototype Pattern Decomposition*

As alluded to previously, the best-rank tensor prototype tensor decomposition allows best trade-off between data compression and recognition accuracy. The only control parameters of the method are requested new rank values for each of the dimensions of the prototype pattern tensor. These, in turn, can be determined experimentally or with one of the heuristic methods usually based on signal energy analysis [5, 13]. In this section, a brief introduction to multilinear analysis and best-rank tensor decomposition is presented. More information on tensors and different types of their decompositions can be found in literature [3, 5, 10, 11].

For further discussion, a tensor $\mathcal{T} \in \Re^{N_1 \times N_2 \times \ldots N_K}$ can be seen as a K-dimensional cube of data, in which each dimension correspond to a different factor of the input data space. With this definition, the j-mode vector of the K-th order tensor is a vector obtained from elements of $\mathcal{T}$ by varying only one its index n_j while keeping all other indices fixed. Further, if from the tensor $\mathcal{T}$ the matrix $\mathbf{T}_{(j)}$ is created, where

$$\mathbf{T}_{(j)} \in \Re^{N_j \times (N_1 N_2 \ldots N_{j-1} N_{j+1} \ldots N_K)}, \tag{1}$$

then columns of $\mathbf{T}_{(j)}$ are *j-mode* vectors of $\mathcal{T}$. Also, $\mathbf{T}_{(j)}$ is a matrix representation of the tensor $\mathcal{T}$, called a j-mode tensor flattening. The j-th index becomes a row index of $\mathbf{T}_{(j)}$, whereas its column index is a product of all the rest K-1 indices. An analysis of sufficient computer representations of (1) are discussed in many publications, for instance in [5].

Further important concept is a p-mode product of a tensor $\mathcal{T} \in \Re^{N_1 \times N_2 \times \ldots N_K}$ with a matrix $\mathbf{M} \in \Re^{Q \times N_p}$. A result of this operation is the tensor $\mathcal{S} \in \Re^{N_1 \times N_2 \times \ldots N_{p-1} \times Q \times N_{p+1} \times \ldots N_K}$ whose elements are obtained based on the following scheme:

$$\mathcal{S}_{n_1 n_2 \ldots n_{p-1} q n_{p+1} \ldots n_K} = (\mathcal{T} \times_p \mathbf{M})_{n_1 n_2 \ldots n_{p-1} q n_{p+1} \ldots n_K} = \sum_{n_p=1}^{N_p} t_{n_1 n_2 \ldots n_{p-1} n_p n_{p+1} \ldots n_K} m_{q n_p}. \tag{2}$$

As was shown, the *p-mode* product can be equivalently represented in terms of the flattened versions of the tensors $\mathbf{T}_{(p)}$ and $\mathbf{S}_{(p)}$. That is, if the following holds

$$\mathcal{S} = \mathcal{T} \times_p \mathbf{M}, \tag{3}$$

then we have the following

$$\mathbf{S}_{(p)} = \mathbf{M}\mathbf{T}_{(p)} \tag{4}$$

In some computations, it is more efficient to represent the tensor and matrix product given in (2) in an equivalent representation based on the p-mode tensor flattening and the Kronecker product. That is,

$$\mathcal{T} = \mathcal{Z} \times_1 \mathbf{S}_1 \times_2 \mathbf{S}_2 \ldots \times_K \mathbf{S}_K, \tag{5}$$

can be equivalently represented as follows

$$\mathbf{T}_{(n)} = \mathbf{S}_n \mathbf{Z}_{(n)} \left[\mathbf{S}_{n+1} \otimes \mathbf{S}_{n+2} \otimes \ldots \otimes \mathbf{S}_K \otimes \mathbf{S}_1 \otimes \mathbf{S}_2 \otimes \ldots \otimes \mathbf{S}_{n-1} \right]^T, \tag{6}$$

where $\otimes$ denotes the Kronecker product between the matrices.

Equipped with the above concepts, the best rank-$(R_1, R_2, \ldots, R_K)$ decomposition of a tensor $\mathcal{T} \in \Re^{N_1 \times N_2 \times \ldots N_K}$ can be defined as a problem of computying a tensor $\tilde{\mathcal{T}}$, which is characteristic of the ranks $rank_1\left(\tilde{\mathcal{T}}\right) = R_1$, $rank_2\left(\tilde{\mathcal{T}}\right) = R_2, \ldots,$ $rank_K\left(\tilde{\mathcal{T}}\right) = R_K$, and which as close as possible approximates to the input tensor $\mathcal{T}$ [11, 12], that is the following functional should be minimized:

$$E\left(\tilde{\mathcal{T}}\right) = \left\| \tilde{\mathcal{T}} - \mathcal{T} \right\|_F^2, \tag{7}$$

where $\|.\|_F$ denotes the Frobenius norm . It can be shown that the approximated tensor $\tilde{\mathcal{T}}$ conveys as much of the "energy", in the sense of the squared entries of a tensor, as the original tensor $\mathcal{T}$, under the requested rank constraints. A value of E is called the reconstruction error. Figure 1 depicts the best rank-(R_1, R_2, R_3) decomposition of a 3D tensor $\mathcal{T} \in \Re^{N_1 \times N_2 \times N_3}$. However, contrary to the rank definition of the matrices, there are different rank definitions for tensors. For more discussion see [5, 11].

It can be also easily observed that the assumed rank conditions mean that the approximation tensor $\tilde{\mathcal{T}}$ can be decomposed as follows

$$\tilde{\mathcal{T}} = \mathcal{Z} \times_1 \mathbf{S}_1 \times_2 \mathbf{S}_2 \ldots \times_K \mathbf{S}_K, \tag{8}$$

Each of the matrices $\mathbf{S}_1 \in \Re^{N_1 \times R_1}$, $\mathbf{S}_2 \in \Re^{N_2 \times R_2}$, ..., and $\mathbf{S}_K \in \Re^{N_K \times R_K}$ in (8) has orthonormal columns. The number of columns for $\mathbf{S}_i$ is given by R_i.

The core tensor $\mathcal{Z} \in \Re^{R_1 \times R_2 \times \ldots \times R_K}$ is of dimensions $R_1, R_2, \ldots, R_K$. It can be computed from the original tensor $\mathcal{T}$ as follows

$$\mathcal{Z} = \mathcal{T} \times_1 \mathbf{S}_1^T \times_2 \mathbf{S}_2^T \ldots \times_K \mathbf{S}_K^T. \tag{9}$$

Summarizing, to find the best rank-$(R_1, R_2, \ldots, R_K)$ approximation of $\mathcal{T}$ it is sufficient to determine only a set of $\mathbf{S}_i$ in (8), and then $\mathcal{Z}$ is computed from Eq. (9).

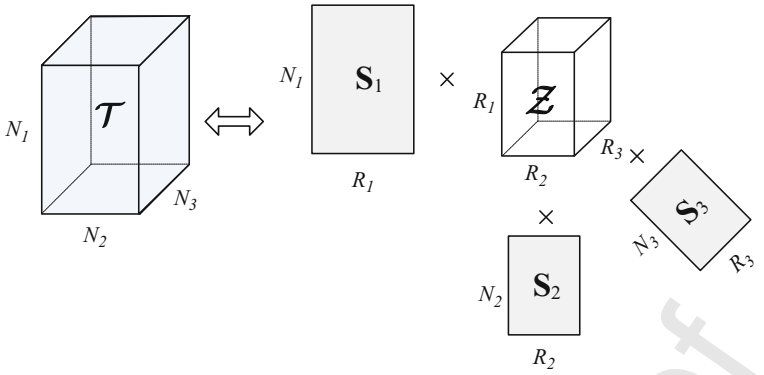

Fig. 1 Schematic representation of the best rank-(R_1, R_2, R_3) decomposition of a 3D tensor

Further analysis is constrained exclusively to 3D tensors, such as the one shown in Fig. 1. It can be seen that this decomposition leads to a significant data reduction. The compression C ratio can be expressed as follows:

$$C = (R_1 R_2 R_3 + N_1 R_1 + N_2 R_2 + N_3 R_3)/(N_1 N_2 N_3). \tag{10}$$

As alluded to previously, the only control parameters of the method are the ranks R_1, R_2, and R_3. A trade-off can be achieved between the compression ratio C in (10) with respect to the approximation error expressed in Eq. (7). This influences also pattern recognition accuracy, as will be discussed.

2.2 *Pattern Classification with the Best Rank Tensor Decomposition*

The already described, the subspace obtained after the best rank decomposition can be used to generate specific features of an image $\mathbf{X}$, which can be then used for pattern recognition [16]. The features are obtained by projecting the image $\mathbf{X}$ of dimensions $N_1 \times N_2$ into the space spanned by the two matrices $\mathbf{S}_1$ and $\mathbf{S}_2$ in accordance with (9). However, at first the pattern $\mathbf{X}$ needs to be represented in an equivalent tensor form $\mathcal{X}$ which is of dimensions $N_1 \times N_2 \times 1$. Then, the feature tensor $\mathcal{F}$ of dimensions $R_1 \times R_2 \times 1$ is obtained by projecting $\mathcal{X}$ onto the space spanned by $\mathbf{S}_1$ and $\mathbf{S}_2$, as follows

$$\mathcal{F}_{\mathbf{X}} = \mathcal{X} \times_1 \mathbf{S}_1^T \times_2 \mathbf{S}_2^T \tag{11}$$

Tensor $\mathcal{T}$ contains is constructed out of the available training patterns. However, the method can work depending on a number of available training patterns, starting from only one exemplar, as will be discussed. Hence, in our framework the following two scenarios were evaluated, depending on the available number of training patterns:

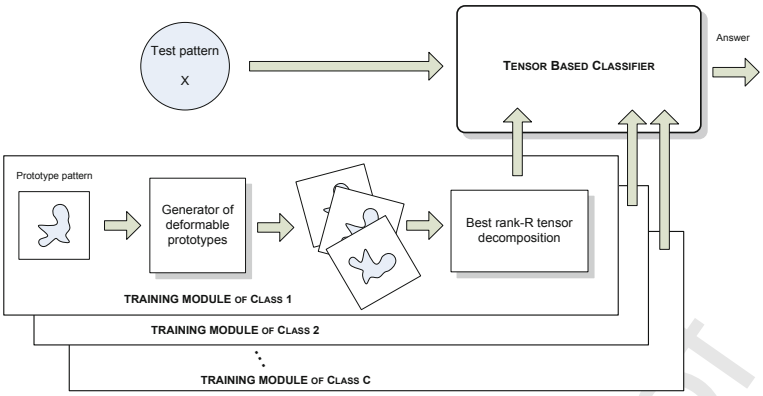

Fig. 2 The process of the 3D pattern tensor generation by geometrical warping of the prototype pattern

1. A set of prototype patterns $\mathbf{P}_i$ of the same object is available. These are used to form the input tensor $\mathcal{T}$.
2. If only one prototype $\mathbf{P}$ is available, its different appearances $\mathbf{P}_i$ are generated by geometrical warping of the available pattern. This process is visualized in Fig. 2.

As a result the patterns form a 3D tensor after the best-rank decomposition spans the space representing that class. In the case of multiple classes, a 3D tensor is built for each of the classes separately.

The next step after the best rank-$(R_1, R_2, \ldots, R_K)$ decomposition consist of building features from each of the prototype patterns $\mathbf{P}_i$ from the tensor $\mathcal{T}$. These are computed as follows

$$\mathcal{F}_i = \mathcal{P}_i \times_1 \mathbf{S}_1^T \times_2 \mathbf{S}_2^T, \tag{12}$$

where $\mathcal{P}_i$denotes an $N_1 \times N_2 \times 1$ tensor representation of the pattern $\mathbf{P}_i$. In the same way features are computed for the tensor $\mathcal{P}_X$ created from the test pattern $\mathbf{P}_X$. It is interesting to notice that dimensions of the computed in this way features are much less than dimensions of the original patterns due to data compression expressed by (10). However, they represent the two-dimensional dominating spaces in each dimension independently. Thus, their discriminative properties are usually high despite low-dimensional representation.

Finally, a quantitative measure of the fitness of the test pattern $\mathbf{P}_X$ to the prototypes of a class c is computed based on the following formula

$$\rho_c = \frac{1}{N_3} \sum_{i=1}^{N_3} \left\| \mathcal{F}_{\mathbf{X}} - \mathcal{F}_i^{(c)} \right\|_F. \tag{13}$$

In a case of a multi-class classification scheme, a best fit class c^* is chosen which minimizes its fitness measure, as follows

$$c^* = \underset{1 \le c \le C}{\arg\min} (\rho_c). \tag{14}$$

Figure 3 depicts the described process of multi-class pattern recognition from the best-rank decomposition of the prototype pattern tensor.

As alluded to previously, the training parameters are the chosen rank values of R_1, R_2, and R_3 in (8). In our experiments these are usually determined experimentally, although they can be also chosen after analyzing signal energy level in the decomposed tensor. However, especially interesting is the case of $R_3 = 1$ which means that the third dimension of the pattern tensor, which reflects a number of training patterns, will be compressed to one the most prominent example. Such strategy frequently leads to superior results, as will be presented in the experimental part.

3 Implementation of the Best Rank Tensor Decomposition

Computation of the best rank-(R_1, R_2, …, R_K) decomposition of tensors, given by Eqs. (8) and (9), can be done with the Alternating Least-Squares (ALS) method, as proposed by Lathauwer et al. [11, 12]. In each step of this method only one of the matrices $\mathbf{S}_k$ is optimized, whereas other are kept fixed [1, 5]. The main concept of this approach is to express the quadratic expression in the components of the unknown matrix $\mathbf{S}_k$ with orthogonal columns with other matrices kept fixed. That is, the following problem is solved

$$\max_{\mathbf{S}_i} \{\Psi\ (\mathbf{S}_i)\} = \max_{\mathbf{S}_i} \left\| \mathcal{T} \times_1 \mathbf{S}_1^T \times_2 \mathbf{S}_2^T \ldots \times_K \mathbf{S}_K^T \right\|^2. \tag{15}$$

Columns of $\mathbf{S}_i$ can be obtained finding the orthonormal basis of the dominating subspace of the column space of the approximating matrix $\hat{\mathbf{S}}_i$. As already mentioned, in each step only one matrix $\mathbf{S}_i$ is computed, while other are kept fixed. Such procedure—called the Higher-Order Orthogonal Iteration (HOOI)—is repeated until the stopping condition is fulfilled or a maximal number of iterations is reached [5, 12]. The pseudo-code of the algorithm is presented in Fig. 4.

In the above algorithm, the function $svds(\hat{\mathbf{S}}, R)$returns the R left leading singular vectors of a matrix $\hat{\mathbf{S}}$. These vectors are orthogonal. Frequently the matrix $\hat{\mathbf{S}}_k$has much more columns c than rows r. In such a case more efficient becomes computation of the *svds* from the product $\hat{\mathbf{S}}_k \hat{\mathbf{S}}_k^T$, instead of the matrix $\hat{\mathbf{S}}_k$using the fact that if a matrix $\mathbf{M} = \mathbf{SVD}^{\mathrm{T}}$, then $\mathbf{MM}^{\mathrm{T}} = \mathbf{SV}^2\mathbf{S}^{\mathrm{T}}$.

Initialization of the matrices in the algorithm in Fig. 4 can be done with the prior HOSVD decomposition. Although such strategy does not guarantee the optimal solution, in practice usually it leads to good results [12]. However, HOSVD is computationally demanding, so for larger problems Wang and Ahuja propose to initialize $\mathbf{S}_k$, either with constant values, or with the uniformly distributed random numbers. These strategies when applied to image processing tasks gave almost the same results as initialization with the HOSVD [16]. Such an initialization method is also recommended in the paper by Chen and Saad [1]. In our software framework, accessible from [7], we also follow this way and initialize $\mathbf{S}_k$ with uniform random generator.

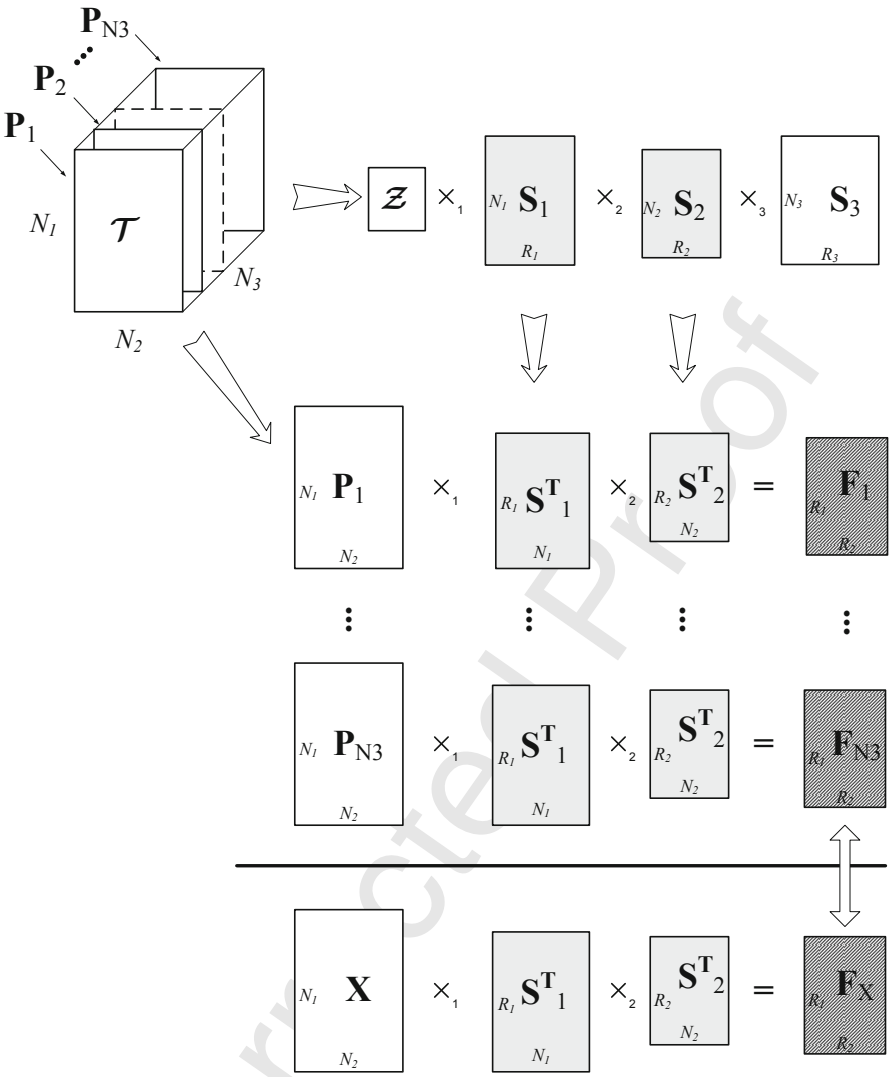

Fig. 3 Pattern recognition scheme with the best rank-(R_1, R_2, …, R_K) decomposition of a tensor composed from the prototype patterns $\mathbf{P}_1$, $\mathbf{P}_2$, …, $\mathbf{P}_{N3}$ of a single class. Decomposition of the pattern tensor provides the lower-dimensional subspaces given by the column orthogonal matrices $\mathbf{S}_1$, $\mathbf{S}_2$, and $\mathbf{S}_3$. Prototype features are obtained by projecting each prototype patterns onto the space spanned by the matrices $\mathbf{S}_1$ and $\mathbf{S}_2$. Features of the test pattern $\mathbf{X}$ are finally compared with the prototype features. The procedure is repeated for each class and the class with the best match of features is returned by the classifier

The above HOOI procedure has been implemented in our software framework, as described in [5]. The implementation utilizes C++ classes with basic data types defined as template parameters, as shown in Fig. 5. This allows time and memory

1. Set a number of ranks $R_1, R_2, \ldots, R_K$.
Set accuracy threshold e_{thresh}

2. Initialize the mode matrices with random values

$$\mathbf{S}_k^{(0)} \in \Re^{N_k \times R_k} \text{ for } 1 \le k \le K$$

$$t = 0$$

3. Do:

4. For each k in range $(1 \le k \le K)$, do:

$$\hat{\mathbf{S}}_k^{(t+1)} = \mathbf{T}_{(k)} \left[\underbrace{\mathbf{S}_{k-1}^{(t)} \otimes \mathbf{S}_{k-2}^{(t)} \otimes \ldots \otimes \mathbf{S}_1^{(t)}}_{F_1} \otimes \underbrace{\mathbf{S}_P^{(t+1)} \otimes \ldots \otimes \mathbf{S}_{k+1}^{(t+1)}}_{F_2} \right]$$

$$\mathbf{S}_k^{(t+1)} = svds\left(\hat{\mathbf{S}}_k^{(t+1)}, R_k\right)$$

$$\mathcal{Z}_{t+1} = \mathcal{T} \times_1 \mathbf{S}_1^{(t+1)^T} \times_2 \mathbf{S}_2^{(t+1)^T} \ldots \times_P \mathbf{S}_P^{(t+1)^T}$$

$$e = \left| \left\| \mathcal{Z}_{t+1} \right\|^2 - \left\| \mathcal{Z}_t \right\|^2 \right|$$

while ($e > e_{thresh}$);

3. Output: a set of matrices $\mathbf{S}_k$.

Fig. 4 A procedure for computation of the best rank-($R_1, R_2, \ldots, R_K$) tensor decomposition

savings by using the fixed point representation of data instead of the floating point. In the presented experiments the 12.12 fixed point representation showed to be sufficient (each data is stored on 3 bytes instead of 8, needed in the case of the floating point representation).

The *Best_Rank_R_DecompFor*, shown in Fig. 5, is the main class for the best-rank tensor decomposition. It is derived from the *TensorAlgebraFor* class which implements all basic operations on tensors, such as the *p*-mode multiplications, discussed in the previous section. Tensors, are represented by objects of the class *TFlatTensorFor* which represents tensors in the flattened form. The *Best_Rank_R_DecompFor* class is accompanied by the *S_Matrix_Initializer* hierarchy. Its main role is to define the way of initial setup of the values of the $\mathbf{S}_i$ matrices for the HOOI process. In our case these were initialized with randomly generated values of uniform distribution [5, 7].

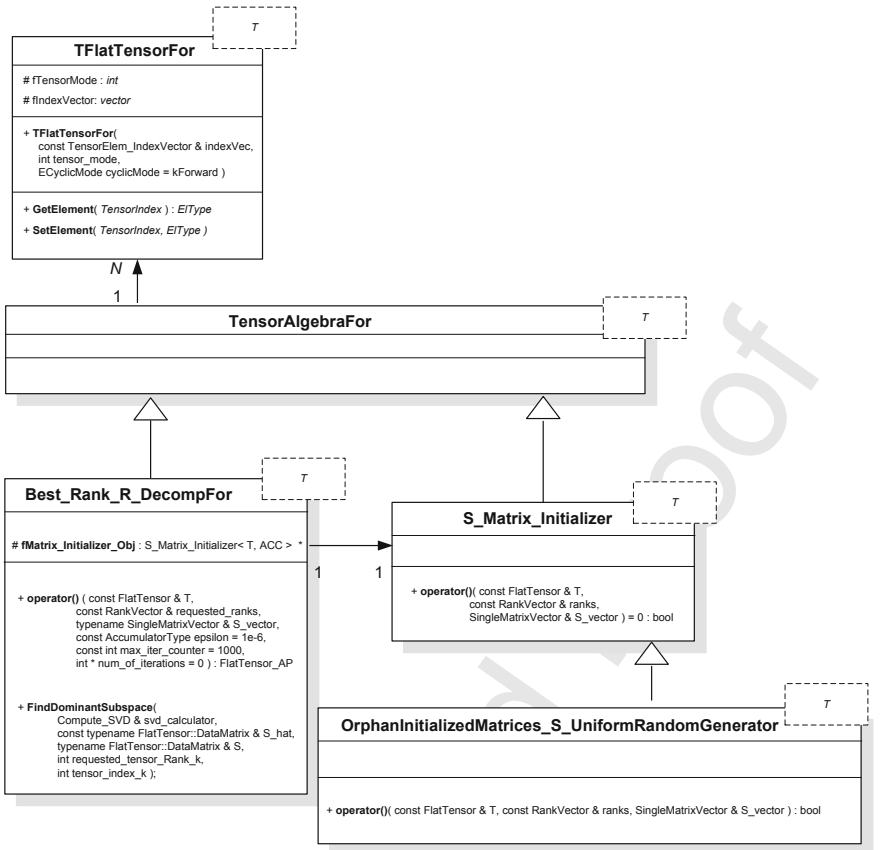

Fig. 5 Class hierarchy from the DeRecLib library implementing the best-rank tensor decomposition for tensors of any dimensions and any type of elements

4 Experimental Results

This paper is based on the previous version, presented in [4]. In this section we cite these results, augmented with results of the tests on face recognition. Figure 6 depicts a maxillary radiograph (left), as well as the implant pattern (right).

In the first task, the implants in the maxillary radiograph images are recognized with the proposed technique. At first, the places of implants are detected by exploiting their high contrast in the radiograph images. These are detected as highly contrast areas, which after registration are fed to the tensor classifier described in the previous sections. Since only one example of the prototype image is usually available, its different appearances are generated by image warping, as described in the previous section. In the experiments an implant pattern is rotated in the range of $\pm 12°$.

Fig. 6 An example of a maxillary radiograph image (**a**) and a dental implant to be recognized (**b**). (Based on [4])

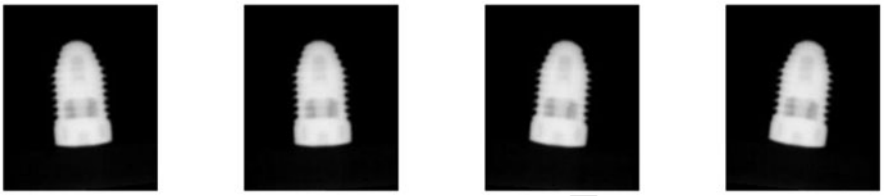

Fig. 7 Examples of the geometrically deformed versions of the prototype image of an implant. These are formed into a 3D tensor which after the best-rank approximation is used in object recognition. (From [4])

Additionally, a Gaussian noise is also added to increase robustness of the method. Examples of deformed versions of the prototype image of an implant are depicted in Fig. 7. These form a 3D tensor which, after the best-rank decomposition, is used in recognition process as already discussed.

Figure 8a shows a plot of the reconstruction error E, expressed in Eq. (7), in respect to the compression ratio C, given in Eq. (10).

In the presented experiments, size of the tensor $\mathcal{T}$ is $56 \times 56 \times 13$. Figure 8b depicts a plot showing accuracy of the pattern recognition, in respect to the compression ratio C. The accuracy with the best representing patter, presented in Fig. 3, allows accuracy at the level of 95–96 %. However, thanks to a different classification method, accuracy level was higher by 1–2 % in the presented experiments. The ranks were chosen 1/4 of the spatial resolution and 1/2 for the pattern dimension of the input tensors. In further research we plan to conduct more extensive comparison of different rank settings, as well as different pattern recognition strategy, in respect to the system accuracy.

In the second group of experiments, the method was tested in the tasks of face recognition. For this purpose the ATT Lab (formerly the ORL Database of Faces) face database were used, examples of which are depicted in Fig. 9. This database contains a set of face images taken in the laboratory conditions [9].

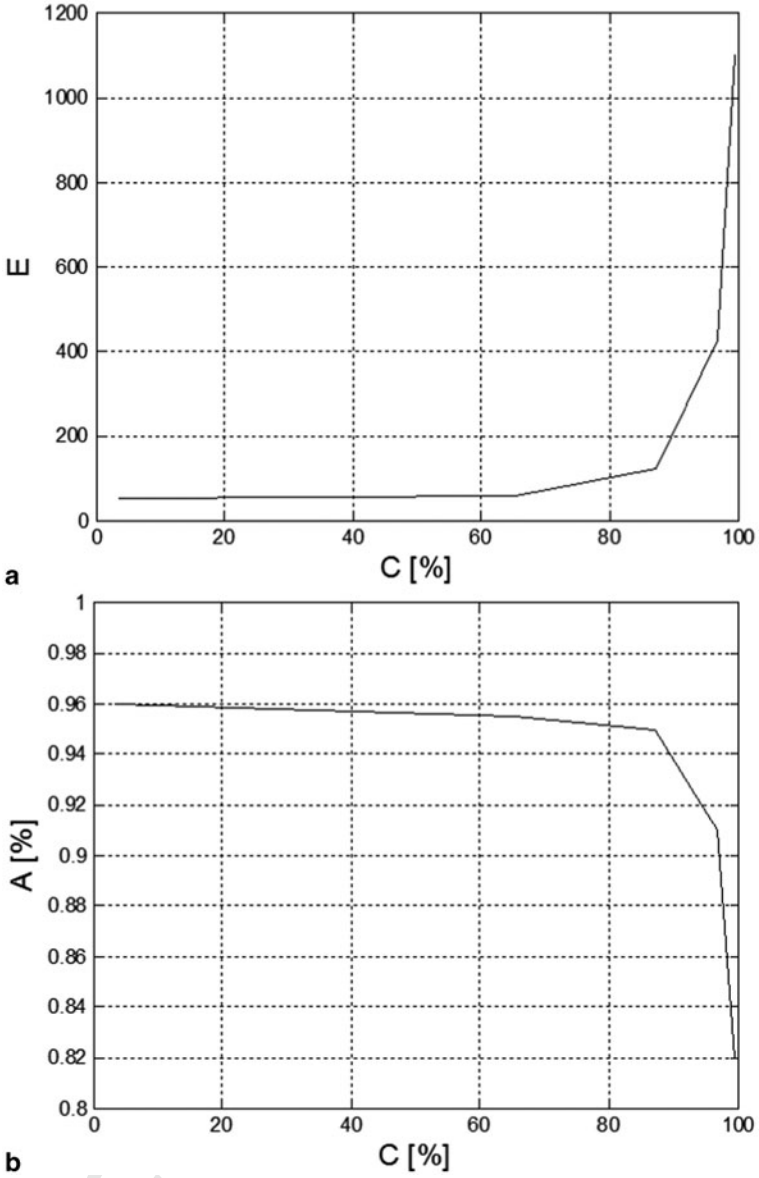

Fig. 8 Reconstruction error E in respect to the compression ratio C of the input patterns (**a**) Accuracy A of pattern recognition in respect to the compression ratio C of the input patterns (**b**). (From [4])

There are ten different images of each of 40 distinct persons. For few subjects, the images were taken at different times, at varying lighting conditions, as well as with different facial expressions (open/closed eyes, smiling/not smiling) and facial

Fig. 9 Examples of the images from the Olivetti Research Lab (ORL)—now ATT Labs. There are 40 subjects, for each there are ten images from which a number were randomly selected for training and the remaining for testing

details (glasses/no glasses). All the images were taken against a dark homogeneous background with the subjects in an upright, frontal position (with tolerance for some side movement).

Figure 10 presents two accuracy plots obtained on the ATT face database with the presented method. In Fig. 10a accuracy is shown in respect to different rank assignments, which directly influence compression ratio, in accordance with formula (10). In this experiment nine images were used for training and the remaining one for testing. The procedure was repeated 10 times. The rank values in Fig. 10a are as follows: (20, 20, 1), (20, 20, 3), (40, 40, 1), (10, 10, 1), (20, 20.9). We notice, that different ranks lead to different accuracy and there is no simple formula joining the compression ration C with accuracy A. Nevertheless, high C leads to lowering A.

In Fig. 10b the same ranks (20, 20,1) are used and the accuracy is drawn in respect to different partitions of the database patterns into the training and testing groups respectively. These are as follows: 9 vs. 1, 7 vs. 3, 5 vs. 5, and 3 vs. 7. Although, a lowering number of training patterns with a higher number of test patterns leads to lower accuracy, the drop is by 0.1 (that is, by 10 %). For future research we plan further investigation, as well as we will try to develop the methods of automatic rank assignments based on signal properties.

The used database is demanding due to high diversity of face appearances within majority of single person. Despite this difficulty, the proposed method allows high accuracy and performs in real-time. Hence, the method can be used in many medical, as well as biometrical on other pattern recognition tasks.

5 Conclusions

The paper presents a framework for pattern recognition in the multi-dimensional image signals with help of the best rank decomposition of the prototype pattern tensors. The tensors are proposed to be formed from the patterns defining a class, either from the statistical group of prototype patterns, or from a series of patterns generated after geometrical transformations of a available single prototype. Pattern recognition

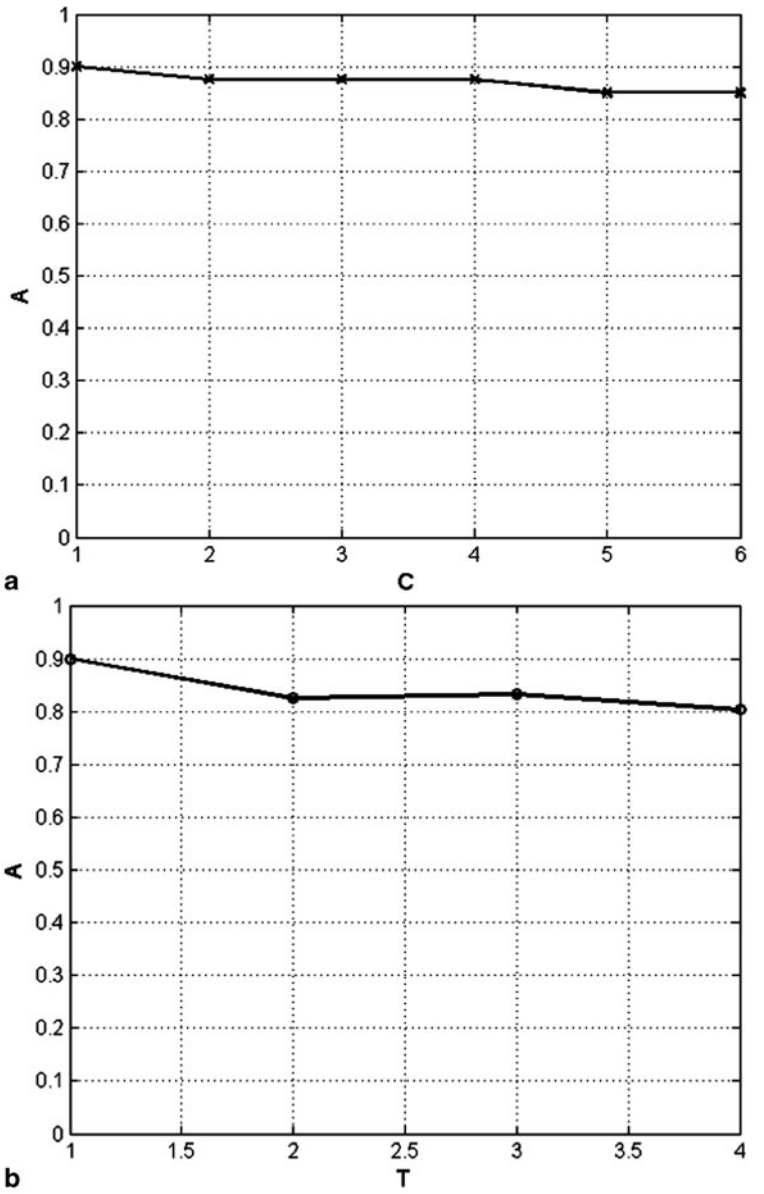

Fig. 10 Accuracy of face recognition in respect to different compression ratio C (**a**). Accuracy of face recognition for the same compression ratio (20, 20, 1) and different assignments T of training vs. testing images (**b**)

is accomplished by testing a distance of the features obtained by projection of the patterns into the best rank tensor subspace and comparing with features of all the projected prototypes. The method was tested on the number of image groups and

showed high accuracy and fast response time. In the presented experiments with implant recognition in maxillary radiograph images, the reached accuracy is 97 %. The method was also tested on the problem of face recognition. In the task of face recognition from the face database the method achieves 90 % accuracy on average. Additionally, the object-oriented software platform was presented which, apart from training computations, allows real time response time. It was also indicated that the training process can be easily parallelized, since each class can be processed independently. The software for tensor decomposition is available from the webpage [7]. Our future research on this subject will concentrate on further analysis, measurement of different signal transformations, as well as on development of methods for best rank assignments.

Acknowledgements The financial support from the Polish National Science Centre NCN in the year 2014, contract no. DEC-2011/01/B/ST6/01994, is greatly acknowledged.

References

1. Chen J, Saad Y (2009) On the tensor svd and the optimal low rank orthogonal approximation of tensors. SIAM J Matrix Anal Appl 30(4):1709–1734
2. Cichocki A, Zdunek R, Amari S (2008) Nonnegative matrix and tensor factorization. IEEE Signal Process Mag 25(1):142–145 **[AQ1]**
3. Cichocki A, Zdunek R, Phan AH, Amari S-I (2009) Nonnegative matrix and tensor factorizations. Applications to exploratory multi-way data analysis and blind source separation. Wiley, Chichester **[AQ2]**
4. Cyganek B (2013) Pattern recognition framework based on the best rank-($R_1, R_2, \ldots, R_K$) tensor approximation. In: Computational vision and medical image processing IV: proceedings of VipIMAGE 2013—IV ECCOMAS thematic conference on Computational vision and medical image processing, pp 301–306
5. Cyganek B (2013) Object detection and recognition in digital images: theory and practice. Wiley **[AQ3]**
6. Cyganek B, Malisz P (2010) Dental implant examination based on the log-polar matching of the maxillary radiograph images in the anisotropic scale space. IEEE Engineering in Medicine and Biology Conference, EMBC 2010, Buenos Aires, Argentina, pp 3093–3096
7. DeRecLib (2013) http://www.wiley.com/go/cyganekobject **[AQ4]**
8. Duda RO, Hart PE, Stork DG (2001) Pattern classification. Wiley, New York
9. https://www.cl.cam.ac.uk/research/dtg/attarchive/facedatabase.html
10. Kolda TG, Bader BW (2008) Tensor decompositions and applications. SIAM Review **[AQ5]**
11. Lathauwer de L (1997) Signal processing based on multilinear algebra. PhD dissertation, Katholieke Universiteit Leuven
12. Lathauwer de L, Moor de B, Vandewalle J (2000) On the best rank-1 and rank-($R_1, R_2, \ldots, R_N$) approximation of higher-order tensors. SIAM J Matrix Anal Appl 21(4):1324–1342
13. Muti D, Bourennane S (2007) Survey on tensor signal algebraic filtering. Signal Process 87:237–249
14. Savas B, Eldén L (2007) Handwritten digit classification using higher order singular value decomposition. Pattern Recognit 40(3):993–1003
15. Wang H, Ahuja N (2004) Compact representation of multidimensional data using tensro rank-one decomposition. In: Proceedings of the 17th international conference on pattern recognition, Vol 1, 4pp 4–47
16. Wang H, Ahuja N (2008) A tensor approximation approach to dimensionality reduction. Int J Comput Vision 76(3):217–229

Chapter 6: Author Query

AQ1. Reference no. 2. 6, 8, 15 are not cited in the text. Please provide the citation.

AQ2. We have updated Ref. 3 and 8. Please check.

AQ3. Please provide the publisher location for Ref. 5.

AQ4. Please provide the access date for Ref. 7 and 9.

AQ5. Please provide complete details for the Ref. 10.